

Observation of Bhabha Scattering in the Center-of-Mass Kinetic-Energy Range 342 to 845 keV

U. von Wimmersperg,^(a) S. H. Connell, R. F. A. Hoernlé, and E. Sideras-Haddad

*University of the Witwatersrand—Council for Scientific and Industrial Research, Schonland Research
Centre for Nuclear Sciences, University of Witwatersrand, Johannesburg 2001, South Africa*

(Received 11 May 1987)

Positions from a ^{27}Si source, obtained through the reaction $^{27}\text{Al}(p,n)^{27}\text{Si}$, were scattered off electrons in a target of polyethylene, and e^+e^- coincidences were detected in a pair of plastic scintillators. The detector apertures were restricted to accept only events corresponding to maximum momentum transfer at center-of-mass angle $\pi/2$. The variation with energy of the corresponding laboratory angle was utilized to obtain the scattering excitation function from the continuous positron spectrum. Center-of-mass kinetic energies in the e^+e^- system covered the range 342 to 845 keV.

PACS numbers: 13.10.+q, 12.20.Fv, 14.80.Pb

In response to a recent proposal¹ that a scalar magnetic (e^+e^-) resonance might be responsible for discrete positron and electron emission lines in heavy-ion collisions, we have measured the excitation function for Bhabha scattering in the center-of-mass kinetic-energy range 342 to 845 keV. This required β^+ energies between 800 and 2400 keV. A suitable source of such positrons is ^{27}Si which provides a β^+ energy spectrum up to 3850 keV with a peak yield around 1700 keV.² The reaction $^{27}\text{Al}(p,n)^{27}\text{Si}$ is convenient for the production of a pure ^{27}Si activity since the only competing process is (p,α) which leads to stable ^{24}Mg . Further advantages are the absence of other aluminum isotopes and the virtually 100% β^+ transition back to the ^{27}Al ground state.³ These features lead to a smooth β^+ energy spectrum and ensure the absence of γ -ray lines other than annihilation at 511 keV.

Positrons emitted from the ^{27}Si source point were collimated to a pencil beam by means of a 1.6-mm-diam canal in a 60-mm-thick lead shield and impinged on a target of polyethylene. Coincidence events between an electron scattered out of the polyethylene target and the positron were detected in a pair of plastic scintillators having the shape of a segmented annulus. The detector apertures were restricted to accept only events corresponding to maximum transfer at center-of-mass angle $\pi/2$. The variation with energy of the corresponding laboratory angle was utilized to obtain the scattering excitation function from the continuous positron spectrum. The associated particles e^+ and e^- are in this case scattered symmetrically through opposite laboratory angles θ and the original energy of the positron can be calculated from

$$\gamma = (3 \cos^2 \theta - 1) / (1 - \cos^2 \theta), \quad (1)$$

where

$$\gamma = W/m \quad (2)$$

is the ratio between the total positron energy and its rest mass. The excitation function for Bhabha scattering was

generated by our progressively moving the annular detector pair along the positron beam axis, thus subtending the series of θ angles required. In addition to simplicity,

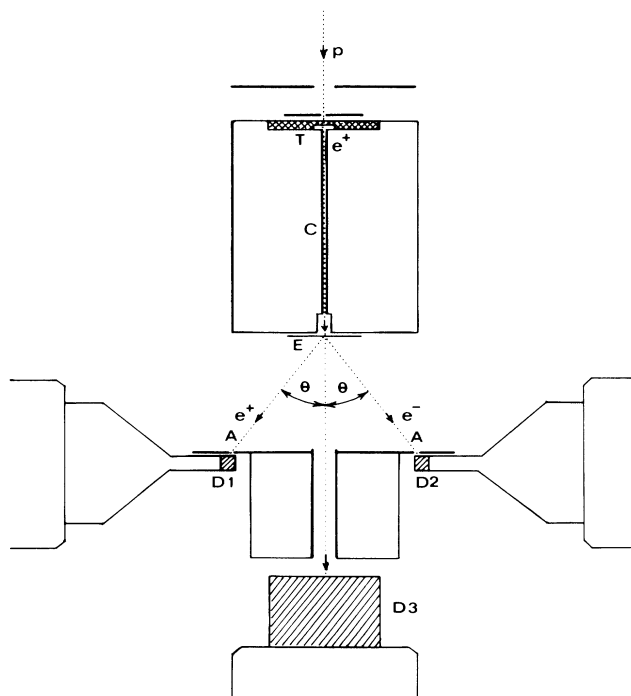


FIG. 1. Schematic section through the target and detector assembly. A chopped beam of 11-MeV protons p produces a source of ^{27}Si in the aluminum target T. A pencil beam of positrons e^+ from ^{27}Si decays is transmitted through a lead shield to polyethylene target E via canal C. Electrons e^- scattered out of E through angle θ , together with the associated positron e^+ , are detected in coincidence by the segmented annular plastic scintillator detectors D1 and D2. The aperture AA is circular and defines the acceptance angle at D1 and D2. Unscattered positrons pass through the central aperture to the plastic scintillator detector D3, which acts as a positron energy-spectrum monitor. Different angles θ (and hence different positron energies) are scanned by locating the three-detector assembly at different axial distances from the electron target E.

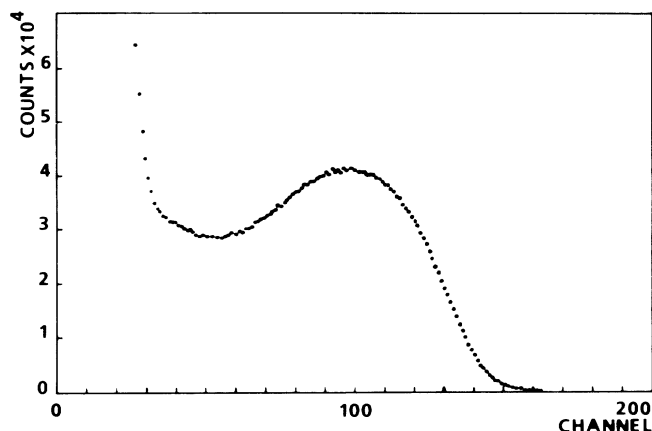


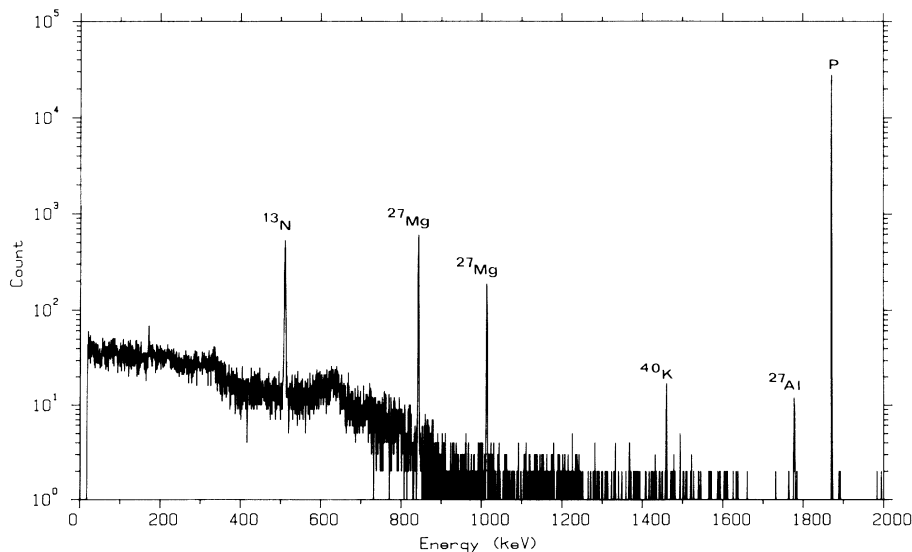
FIG. 2. Positron spectrum from D3.

this method also provides an absolute energy calibration to the accuracy with which θ is defined.

In Fig. 1 we show a schematic view of the positron source, target, and detector arrangement. A beam of 11-MeV protons, from the tandem van de Graaff accelerator at the Schonland Research Centre, irradiated a 1.6-mm-diam spot on the aluminum target T. The proton irradiation was cycled in a repeated sequence of 15 s beam on and 15 s beam off, so as to utilize the 4.2-s half-life decays from ^{27}Si efficiently, while excluding neutron-induced events. Coincidence events in D1 and D2 were collected only during the last 14 s of the beam-off period, allowing 1 s for detector recovery from the neutron irradiation. The 0.8 mm thickness of the aluminum target was chosen to just stop 11-MeV protons even with maximum range straggle. A third detector D3,

thick enough to stop 4-MeV positrons, was used to monitor the actual energy spectrum of positrons transmitted through the electron target E (polyethylene) during each θ run. Absorption and energy-spreading effects in the ^{27}Si source embedded within the aluminum were thus accounted for directly. In Fig. 2 we show the ^{27}Si β^+ spectrum as seen by detector D3. The low-energy background is due to Compton electrons ejected by annihilation radiation. Except for the lowest-energy point, the part of the β^+ spectrum used in our measurements corresponded to the background-free region. A Kurie plot was used to determine the position of the 3850-keV endpoint energy. The β^+ spectrum was then fitted by a skewed Gaussian in order to parametrize yields at the chosen energies.

During preparatory runs for this experiment we became aware of the stringent requirements for purity of the aluminum target. Even trace contamination by other elements can build up unacceptable levels of long-lived activities during several weeks of proton irradiation, averaging 0.15 μA into the 1.6-mm spot. A sample produced as a standard for reactor-grade aluminum eventually proved to be adequate. A Ge(Li) γ -ray spectrum taken after proton irradiation of this sample is shown in Fig. 3. The only contamination detected is a surface layer of oxygen, as evidenced by an annihilation line of 10-min half-life from $^{16}\text{O}(p,\alpha)^{13}\text{N}$. The ^{27}Mg and ^{28}Al lines are due to (n,p) and (n,γ) secondary reactions in the aluminum itself. All the lines are comparable in intensity to a ^{40}K environmental background. The proton collimators were made of high-purity tantalum and contribute only low-energy background through tantalum x rays from electron capture following $^{181}\text{Ta}(p,n)^{181}\text{W}$. We conclude that we have reduced background effects to

FIG. 3. Ge(Li) spectrum from the ^{27}Al target after proton irradiation. P is a calibration pulser line.

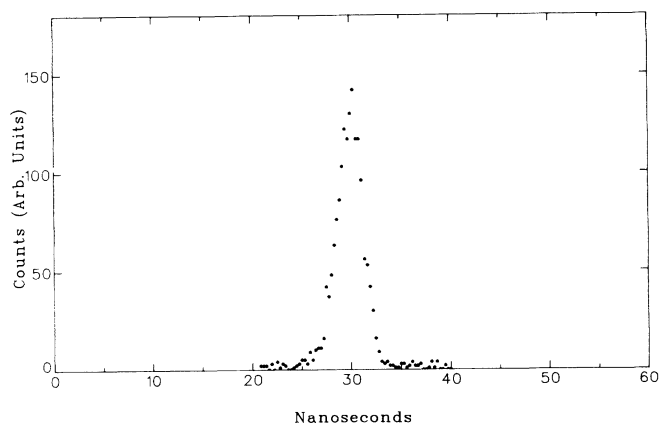


FIG. 4. Time spectrum of D1 and D2 coincidences.

an acceptable level by inspection of the D1 and D2 coincidence time spectrum (Fig. 4), which shows that real coincidences stand out on a negligible background of randoms. Equally satisfying is the featureless character of the β^+ spectrum over the energy region of interest (Fig. 2).

In Fig. 5 we show the number of e^+e^- coincidence events as a function of the center-of-mass kinetic energy

$$\Delta = 2m \{[(\gamma+1)/2]^{1/2} - 1\} \quad (3)$$

normalized to the integrated proton charge received within the 1.6-mm spot on the aluminum target. The

$$\frac{d\sigma}{d\Omega} = \frac{4\pi e^4}{m^2} \left(\frac{\gamma+3}{\gamma+1} \right)^{3/2} \left\{ (\gamma-1)^{-2} + (\gamma-1)^{-1} + \frac{5}{8} + [3(\gamma-1)^{-2} + 2(\gamma-1)^{-1} + \frac{1}{4}] \left[\frac{1}{4} \left(\frac{\gamma-1}{\gamma+1} \right)^2 - \frac{1}{2} \left(\frac{\gamma-1}{\gamma+1} \right) \right] \right\}.$$

The energy resolution inherent in the positron-beam divergence and spot size at the polyethylene target, together with target thickness (0.75 mm) and detector aperture, is 80 keV in the laboratory. The error bars in Fig. 5 reflect statistics. In Fig. 6 we show the results reduced to the Bhabha-scattering cross section.

The $(5.8 \pm 2.7)\%$ deviation from the Bhabha fit at $\Delta = 710$ keV amounts to 14.5 ± 6.8 keV b and has a center-of-mass width of 30 keV, which in the laboratory system is just in excess of our estimated resolution. The mass excess of 710 keV is compatible with the energy of the positron and electron lines observed in heavy-ion scattering within the energy resolution quoted,⁵⁻⁷ but does not agree with Wong and Becker's calculation of 558 keV. Considering the prominence of the discrete e^+e^- lines observed in heavy-ion scattering (of order 50% of the peak plus continuum sum),⁵ our observation of a 6% effect could only be considered as a possible source of these lines if a special mechanism favoring the production of such a resonance can be shown to exist in the environment of heavy-ion collisions.

The authors acknowledge the encouragement of J.P.F. Sellschop and the support of the Council for Scientific and Industrial Research. Our thanks for technical assistance are due to A. E. Pillay, J. U. M. Beer, I. D.

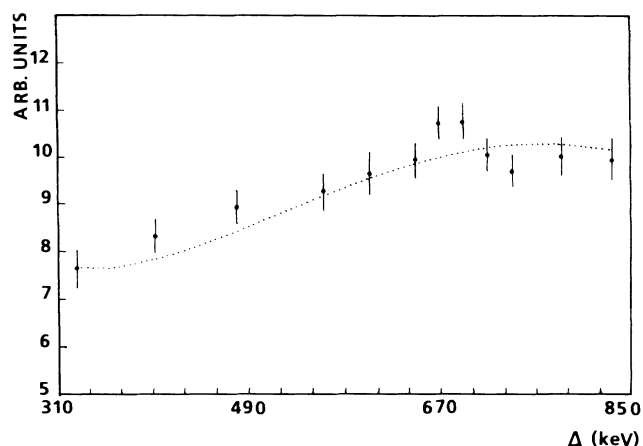


FIG. 5. D1 and D2 coincidences vs kinetic energy in the e^+e^- center-of-mass system. The broken line is calculated with use of the Bhabha cross section and the shape of the positron energy spectrum from detector D3. The error bars are statistical.

curve is a calculation of the yield of e^+e^- coincidences:

$$Y = PN^-(d\sigma/d\Omega)\Delta\Omega, \quad (4)$$

where $P(\gamma)$ is the ^{27}Si source yield of positrons, N^- is the area density of electrons in the polyethylene target, $\Delta\Omega(\gamma)$ is the solid angle subtended at the aperture of detectors D1 and D2, and $d\sigma/d\Omega$ is the differential cross section⁴ for scattering into center-of-mass angle $\pi/2$:

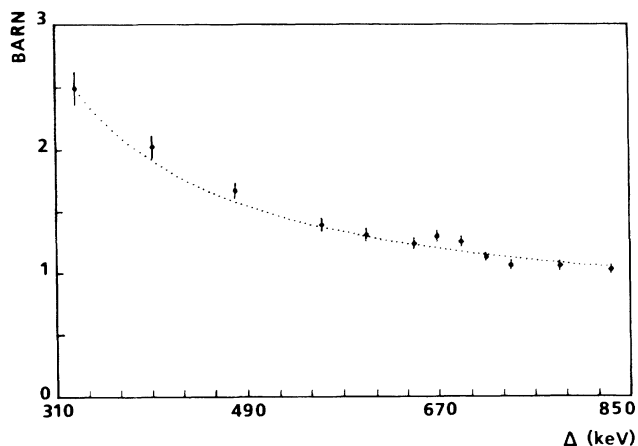


FIG. 6. Bhabha cross section extracted from data of Fig. 5.

McOwen, I. D. McQueen, M. Rebak, and H. Andeweg.

^(a)Now at Accelerator Development Department, Brookhaven National Laboratory, Upton, NY 11973.

¹Cheuk-Yin Wong and R. L. Becker, Phys. Lett B **182**, 251 (1986).

²R. Wallace and J. A. Welch, Jr., Phys. Rev. **117**, 1297 (1960).

³*Table of Isotopes*, edited by C. M. Lederer and V. S. Shirley (Wiley, New York, 1978), 7th ed.

⁴H. J. Bhabha, Proc. Roy. Soc. London A **154**, 195 (1935).

⁵T. Cowan *et al.*, Phys. Rev. Lett. **56**, 444 (1986).

⁶F. Bosch and B. Müller, in *Particle and Nuclear Physics*, edited by A. Faessler (Pergamon, Oxford, 1986), Vol. 16, p. 195.

⁷H. Bokemeyer *et al.*, Gesellschaft für Schwerionenforschung Report No. 85-1, 1985 (unpublished), p. 177.